

Dalton Transactions

Accepted Manuscript



This is an *Accepted Manuscript*, which has been through the RSC Publishing peer review process and has been accepted for publication.

Accepted Manuscripts are published online shortly after acceptance, which is prior to technical editing, formatting and proof reading. This free service from RSC Publishing allows authors to make their results available to the community, in citable form, before publication of the edited article. This *Accepted Manuscript* will be replaced by the edited and formatted *Advance Article* as soon as this is available.

To cite this manuscript please use its permanent Digital Object Identifier (DOI®), which is identical for all formats of publication.

More information about *Accepted Manuscripts* can be found in the [Information for Authors](#).

Please note that technical editing may introduce minor changes to the text and/or graphics contained in the manuscript submitted by the author(s) which may alter content, and that the standard [Terms & Conditions](#) and the [ethical guidelines](#) that apply to the journal are still applicable. In no event shall the RSC be held responsible for any errors or omissions in these *Accepted Manuscript* manuscripts or any consequences arising from the use of any information contained in them.

Characterization of Nickel(II)-Acylperoxo Species Relevant to [View Article Online](#)
Catalytic Alkane Hydroxylation by Nickel Complex with *m*CPBA

Shiro Hikichi,^{*a} Kento Hanaue,^a Takako Fujimura,^a Hideho Okuda,^a Jun Nakazawa,^a
Yoshiko Ohzu,^b Chiho Kobayashi^b and Munetaka Akita^b

^a Department of Material and Life Chemistry

Faculty of Engineering

Kanagawa University

3-27-1 Rokkakubashi, Kanagawa-ku, Yokohama 221-8686 (Japan)

Fax: +81-45-413-9770

E-mail: hikichi@kanagawa-u.ac.jp

^b Chemical Resources Laboratory

Tokyo Institute of Technology

4259 Nagatsuta, Midori-ku, Yokohama 226-8503 (Japan)

Abstract[View Article Online](#)

Nickel complexes with hydrotris(pyrazolyl)borate (= Tp^R) ligands catalyze alkane oxidation with organic peroxide *meta*-Cl-C₆H₄C(=O)OOH (= *m*CPBA). The electronic and steric hindrance properties of Tp^R affect the catalyses. The complex with an electron-withdrawing group containing a less-hindered ligand, that is Tp^{Me₂,Br}, exhibits higher alcohol selectivity. Higher selectivity for secondary over tertiary alcohols upon the oxidation of methylcyclohexane indicates that the oxygen atom transfer reaction proceeds within the coordination sphere of the nickel centers. Reaction of the catalyst precursor, dinuclear nickel(II)-bis(μ -hydroxo) complexes, with *m*CPBA yields the corresponding nickel(II)-acylperoxo species, as have been characterized by spectroscopy. Thermal decomposition of the nickel(II)-acylperoxo species in CH₂Cl₂ yields the corresponding nickel(II)-chlorido complexes through Cl atom abstraction. Employment of the brominated ligand increases the thermal stability of the acylperoxo species. Kinetic isotope effects observed on the decay of the nickel(II)-acylperoxo species indicate concerted O–O breaking of the nickel-bound acylperoxide and H-abstraction from the solvent molecule.

Introduction

[View Article Online](#)

Selective partial oxidation of alkanes to the corresponding alcohols is an important fundamental chemical transformation.¹ In order to achieve high alcohol selectivity, free radical-contributed reaction will give a mixture of alcohol and the corresponding over-oxidized product (i.e. ketone or aldehyde) through the Russel termination mechanism.^{2,3} It therefore remains important to design catalysts that provide a metal-based oxidant showing alkane hydroxylation activity. The most considerable metal-based oxidants are high-valent metal-oxo (or metal-oxyl radical) species. Metal-peroxo species, LM-OO-Z (where L denotes a metal supporting ligand, Z = none, H, alkyl, acyl, metal), are also possible candidates for the metal-based oxidants. Moreover, these species are promising precursors for the metal-oxo species produced by O–O bond activation under mild conditions.⁴

Recently, some experimental^{5–9} and theoretical^{10,11} investigations have revealed the alkane hydroxylation potential of active oxygen complexes of nickel. One of the interesting findings is the selective hydroxylation of cyclohexane catalyzed by nickel(II) complexes with *m*CPBA explored by Itoh and coworkers.^{5a–c} In addition, Balamurugan *et al.* have reported similar catalytic alkane hydroxylation by a series of nickel(II) complexes with *m*CPBA.^{5d} The correlation between the structures of the metal-supporting ligands (shown in Figure 1) and the catalytic activities of the resulting nickel(II) complexes has been revealed. During the catalytic process, homolytic O–O bond rupture of a putative nickel(II)-acylperoxo intermediate occurs, as has been evidenced by the formation of chlorobenzene from *m*CPBA. Although no reaction intermediates have been detected in these catalytic systems, a related mononuclear nickel(III)-oxygen (oxo and hydroxo) species that is formed through the reaction of the Ni(II) precursor with *m*CPBA has very recently been characterized.⁶

In this study, hydrotris(3,5-dialkyl-4-X-pyrazolyl)borates, $\text{Tp}^{\text{R}2,\text{X}}$ where R = Me or *i*Pr and X = H or Br (when X = H, H is omitted in the abbreviation shown as $\text{Tp}^{\text{R}2}$; the abbreviation system follows that in the literatures¹²: see Fig. 1), have been employed as

the nickel-supporting scaffold. The advantage of $\text{Tp}^{\text{R}2,\text{X}}$ is structural and electronic controllability.¹² In particular, substituent groups on the distal fourth position of the pyrazolyl groups affect the electronic nature of the resulting $\text{Tp}^{\text{R}2,\text{X}}$ complex, although the structural environment around the metal center is almost same as that of the prototype compound where $\text{X} = \text{H}$. Such electronic tuning leads to control of the stability and reactivity of the nickel(II)-alkylperoxo species.¹³ This strategy is expected to provide insight into the catalytic alkane hydroxylation mechanism of the nickel(II)/*m*CPBA system. As reported herein, we have explored the catalyses of the $\text{Tp}^{\text{R}2,\text{X}}$ supported nickel(II) complexes toward cyclohexane oxygenation with *m*CPBA. Notably, we have succeeded in detecting thermally unstable nickel(II)-acylperoxo species formed by reaction of the dinuclear nickel(II)-bis(μ -hydroxo) complexes, $[\text{Ni}^{\text{II}}\text{Tp}^{\text{R}2,\text{X}}]_2(\mu\text{-OH})_2$ ($\mathbf{1}^{\text{X}}$ where $\text{R} = \text{Me}$ and $\mathbf{1}'^{\text{X}}$ where $\text{R} = i\text{Pr}$, respectively),^{8e,13,14} with *m*CPBA. Products analyses and kinetic studies of the thermal decomposition process of the nickel(II)-acylperoxo species provide insights into the alkane hydroxylation mechanism through the O–O activation process.

[Fig. 1]

Results and Discussion

Correlation between catalytic activity and the nature of the metal-supporting ligands

Prior to characterization of a putative nickel(II)-acylperoxo intermediate, trends in cyclohexane oxygenation catalyses of the $\text{Tp}^{\text{R}2,\text{X}}$ -supported nickel complexes were explored (Table 1). The catalysts derived from $\mathbf{1}^{\text{X}}$, of which the metal-supporting ligands were the less hindered $\text{Tp}^{\text{Me}2,\text{X}}$, yielded the alcohol as the major product. The more hindered $\text{Tp}^{i\text{Pr}2,\text{X}}$ ligand analogues $\mathbf{1}'^{\text{X}}$ did not exhibit such catalytic activity even in the large excess substrate reaction. In contrast, the alkylperoxonickel(II) complex $[\text{Ni}^{\text{II}}(\text{OO}t\text{Bu})\text{Tp}^{i\text{Pr}2}]$ can catalyze the oxygenation of cyclohexane with

tert-butylhydrogenperoxide, but the major product is cyclohexanone because the free-radical reaction occurs predominantly.⁷ As reported previously by Nam and coworkers, a simple nickel(II) salt (= an MeCN solution of Ni(ClO₄)₂) cannot catalyze cyclohexane oxidation with *m*CPBA.¹⁵ Therefore, the catalytic hydroxylation activity of nickel emerges from employment of the appropriate ligands controlling the generation of a metal-based oxidant. In the case of the tris(pyridylmethyl)amine (= TPA) ligand system, a cobalt catalyst exhibits selective hydroxylation activity similar to that of the nickel catalyst.^{5a} Moreover, a cobalt-porphyrinato complex as well as cobalt-perchlorate salt catalyze cyclohexane hydroxylation with *m*CPBA.^{15,16} In contrast, the cobalt(II) analogues of **1^X** were almost inactive in the examined reaction conditions. These findings imply that the combination of a central metal ion and its supporting ligand is dominant.

[Table 1]

The electron-withdrawing bromine-containing Tp^{Me₂,Br} ligand catalyst **1^{Br}** showed a higher alcohol yield than that of the non-brominated ligand catalyst **1^H** when the reaction proceeded in CF₃C₆H₅ (Figure S4). In the reaction of the mixture of large excess substrate and a small amount of CH₂Cl₂ as solvent for *m*CPBA, the extremely high A/K value (= 53) was achieved by **1^{Br}**. In this reaction condition, TON of **1^{Br}** reached 42 (theoretical maximum is 50). The less electron-withdrawing ligand catalyst **1^H** exhibited somewhat higher TON (= 46) but lower A/K (= 32) (Fig. 2).

[Fig. 2]

Formation of chlorobenzene (= C₆H₅Cl) indicated that homolytic O–O bond cleavage of a putative nickel(II)-acylperoxo intermediate occurred in the present oxidation process.^{5b,d} In the reactions of large excess substrate (entries 3 and 4 in Table 1), 57 μmol of C₆H₅Cl formed when **1^{Br}** was used as the catalyst precursor, while 84 μmol of C₆H₅Cl formed when **1^H** used. The yield of C₆H₅Cl seems to be correlated with the selectivity of the oxygenated products; a small amount of radical species such

as a phenyl radical (generated by decarboxylation of acyloxy radical) might work as a mediator for a free-radical contributed reaction giving a ketone. [View Article Online](#)

When methylcyclohexane was employed as a substrate, $\mathbf{1}^X/m\text{CPBA}$ systems showed high secondary alcohol selectivity (Table 2). In the absence of $\mathbf{1}^X$, i.e. control reactions (entries 3 and 4 in Table 2), the tertiary C–H bond was oxidized selectively. In the case of substituted cyclohexanes, the tertiary C–H is sterically crowded. Therefore, the bulkiness of the oxidant affects the products selectivity¹⁷, and selective hydroxylation on secondary C–H bonds results from sterically demanding $\text{Tp}^{\text{Me}_2, \text{X}}$ -supported nickel-based oxidant.

[Table 2]

To clarify the nature of the active oxygen species, cyclohexane oxidation in the presence of H_2^{18}O was examined. No ^{18}O -labeled cyclohexanol could be detected, whereas an ^{18}O -labeled cyclohexanone was obtained (Fig. S5). These findings imply that the ^{18}O -labeled ketone is not formed from the corresponding alcohol by its over-oxidation, and that the formation pathways of alcohol and ketone are different in our $\text{Tp}^{\text{R}_2, \text{X}}$ -supported nickel-*m*CPBA system as well as the previously reported nickel complexes with the amine-based neutral ligands.⁵ In addition, the oxygen atom of the alkane hydroxylating active species of our system (i.e. nickel-oxygen species) is not exchangeable with the oxygen atom of the water molecule. Incorporation of the oxygen atom of H_2O into cyclohexanol occurs in the cyclohexane oxidation with *m*CPBA catalyzed by iron- and cobalt catalysts (porphyrinato complexes of iron and cobalt, and $\text{Co}^{\text{II}}(\text{ClO}_4)_2$) reported by Nam and coworkers.^{15,16,18} In these iron and cobalt systems, high-valent metal-oxo species are proposed as the active oxidant and their oxo ligands are exchangeable. Such a difference between our nickel and the other systems may be due to the reaction mechanism and the character of the active species. Possible explanations for our nickel system are, (i) the active oxidant is a putative nickel-oxygen species (such as $\text{Ni}^{\text{III}}=\text{O}$ or $\text{Ni}^{\text{II}}-\text{O}\cdot$)^{5b,d,6} and its oxygen atom is readily transferred to the substrate *via* hydrogen atom abstraction and radical-rebound

mechanism, and (ii) a nickel(II)-*m*CPBA complex is the active oxidant and the reaction occurs *via* a concerted mechanism through concomitant O–O rupture and oxygen atom transfer. In the iron-heme system reported by Nam and coworkers, the extent of the ^{18}O incorporation into the product is varied depending on the nature of the catalysts as well as the reaction conditions, including the choice of solvent.¹⁸

Characterization of nickel(II)-acylperoxo species 2^{X}

The alkane hydroxylation catalyses of 1^{X} motivate us to characterize a putative nickel-acylperoxo species that may be a key intermediate formed during the *m*CPBA activation process. Titration of the reaction of 1^{H} with *m*CPBA at 223 K monitored by UV/Vis spectra revealed that increase in the absorption band around 386 nm became saturated when two equivalents of *m*CPBA were added to the CH_2Cl_2 solution of dinuclear nickel(II)-bis(μ -hydroxo) complex 1^{H} (Fig. 3 and Table 3). The intensity of this band is not very high, and the spectral pattern of this pale blue solution is clearly different from those of the dinuclear nickel(III)-bis(μ -oxo) and mononuclear nickel(II)-alkylperoxo complexes with Tp^{R} .^{7,8e,13}

[Fig. 3]

[Table 3]

An IR spectrum of this solution exhibited a peak at 1644 cm^{-1} under a low-temperature condition, and this peak disappeared in response to increases in the solution temperature (Fig. 4). Therefore, the thermally unstable pale blue species could be assigned as the nickel(II)-acylperoxo complex, $[\text{Ni}^{\text{II}}(\text{OOC}(=\text{O})\text{C}_6\text{H}_4\text{Cl})(\text{Tp}^{\text{Me}_2})]$ (2^{H}), formed through dehydrative condensation of 1^{H} with a stoichiometric amount of *m*CPBA (i.e., $\text{Ni(II):mCPBA} = 1:1$).¹⁹ The $\nu\text{C}=\text{O}$ bands of free *m*CPBA and *m*CBA are observed at 1738 and 1706 cm^{-1} , respectively, under the same condition (i.e. CH_2Cl_2 solution at 223 K). To date, a few *meta*-chloroperbenzoate complexes have been characterized, and the wavenumbers of their $\nu\text{C}=\text{O}$ bands (observed in the solid state) are correlated to the binding mode of the

acylperoxo moieties, as summarized in Table 4.^{20–22} As found for the structure-determined dinuclear copper(II) complex, the non-coordinating acyl group shows a small blue shift of the $\nu\text{C}=\text{O}$ compared to that of the free *m*CPBA.²¹ The observed $\nu\text{C}=\text{O}$ peak at 1644 cm^{-1} of **2^H** suggests coordination of the acyl group to the nickel center (see Scheme 1), and the molecular structure of **2^H** is probably similar to that of the copper(II) derivative of $\text{Tp}^{i\text{Pr}2}$ reported by Kitajima and coworkers.²²

[Fig. 4]

[Table 4]

The other nickel(II)-hydroxo complexes, not only the catalytically active $\text{Tp}^{\text{Me}2,\text{Br}}$ but also the inactive $\text{Tp}^{i\text{Pr}2,\text{X}}$ derivatives, gave the corresponding acylperoxo complexes **2^{Br}** and **2^X**, respectively. As summarized in Tables 3 and 4, spectral patterns of UV/Vis and wavenumbers of $\nu\text{C}=\text{O}$ of **2^{Br}** and **2^X** are similar to those of **2^H**. These findings indicate that the reason for the catalytic inertness of the $\text{Tp}^{i\text{Pr}2,\text{X}}$ complexes is the steric hindrance between the substrate and the *isopropyl* groups surrounding the nickel center. Three *isopropyl* groups on the third position of the pyrazolyl rings in $\text{Tp}^{i\text{Pr}2,\text{X}}$ work as hindered shades surrounding the nickel center, which stabilizes the nickel(II)-acylperoxo species. In fact, the most stable complex **2^{Br}** could be isolated, although the C–H hydroxylation potential was retained, as evidenced by the intra-molecular ligand oxygenation (*vide infra*). Unfortunately, our challenge to get single crystals of **2^{Br}** (and other ligands derivatives) has not met with success thus far.

Characterization of product complexes derived from thermal decomposition of **2^X** and **2^X**

The nickel(II)-acylperoxo species **2^X** and **2^X** decomposed even at 253 K, and the resulting product nickel(II) complexes were varied depending on conditions such as solvent and temperature as well as R of $\text{Tp}^{\text{R}2,\text{X}}$ (Scheme 1).

[Scheme 1]

(i) **Products from the $\text{Tp}^{\text{Me}2,\text{X}}$ complexes **2^X**.** In the case of the CH_2Cl_2 solution

of 2^X having the less hindered $\text{Tp}^{\text{Me}2,X}$, raising the solution temperature from 223 to 253 K resulted in changing the solution color from pale blue-green to pale brown. The resultant pale brown solutions exhibited absorption around 480 nm attributed to the Cl-to-Ni charge transfer band of nickel(II)-chloride complexes, $[\text{Ni}^{\text{II}}(\text{Cl})(\text{Tp}^{\text{Me}2,X})]$ (3^X ; see Fig. 5(a): the formed complexes 3^X were characterized by comparison to authentic samples synthesized via another method).²³ The yields of 3^X were over 85 % (determined by UV/Vis) when the CH_2Cl_2 solutions of 2^X were stored at 253 K for 12 h and then slowly warmed to room temperature. As we have reported previously, thermal decomposition of the nickel(II)-*tert*-butylperoxo complexes with $\text{Tp}^{i\text{Pr}2,X}$ in CH_2Cl_2 yields the corresponding chloride complexes $[\text{Ni}^{\text{II}}(\text{Cl})(\text{Tp}^{i\text{Pr}2,X})]$ (3^X) with moderate yield (ca 30 %).^{7,13} The formation of 3^X may proceed through abstraction of the Cl atom from CH_2Cl_2 by a putative nickel(I) species given by the Ni–O bond homolysis of the alkylperoxo complexes. The yielding of 3^X from the nickel(II)-acylperoxo complexes 2^X suggests the formation of a nickel(I) species through the thermal decomposition process. Itoh and coworkers have proposed formation of the nickel(I) species after the hydroxylation of alkane in the catalytic processes.^{5b} In this context, we can hypothesize that nickel(I) species with $\text{Tp}^{\text{Me}2,X}$ are formed after the oxidation of CH_2Cl_2 . The formation rates of 3^X (3.2×10^{-4} for 3^{H} and $5.2 \times 10^{-5} \text{ s}^{-1}$ for 3^{Br} , respectively, at 253 K) were lower than the decay rates of the corresponding 2^X (*vide infra*). Therefore, the conversion from 2^X to 3^X might proceed by a stepwise process through the decomposition of 2^X and following reaction of the resulting nickel(I) species with CH_2Cl_2 to give 3^X , although we have not succeeded in trapping any intermediates so far.

Other products in the decomposition reactions in CH_2Cl_2 were nickel(II)-*meta*-chlorobenzoate complexes, $[\text{Ni}^{\text{II}}(\text{O}_2\text{CC}_6\text{H}_4\text{Cl})(\text{Tp}^{\text{Me}2,X})]$ (4^X), having characteristic absorption bands around 420–430 nm (see experimental section). Decomposition of 2^X in CH_2Cl_2 at 273 K led to an increase in the yield of 4^X with decreases in 3^X , as shown in Fig. 5(b). Therefore, the formation of 3^X and 4^X occurred

competitively.

[View Article Online](#)

[Fig. 5]

Decomposition of 2^X in toluene yielded 4^X , with yields of 4^H and 4^{Br} of 73 and 77 % (determined by UV/Vis), respectively. A possible explanation for the formation of 4^X is coupling of the nickel(I) species with acyloxy radical resulting from homolysis of the O–O bond of 2^X (see Scheme 2). Mass spectral analyses revealed no formation of oxidized $Tp^{Me_2,X}$ ligands compounds in the case of products derived from either CH_2Cl_2 or toluene solutions. However, decomposition of 2^{Br} in CD_2Cl_2 resulted in the oxidation of $Tp^{Me_2,Br}$. This result implies that there are competitive reactions between the solvent and the methyl group on $Tp^{Me_2,Br}$.

(ii) Ligand hydroxylation on $Tp^{iPr_2,X}$ complexes 2^X . In the case of more hindered $Tp^{iPr_2,X}$ systems, the solvent type did not affect the products. UV-vis spectra of the products derived from both CH_2Cl_2 and Et_2O solutions of 2^X exhibited peaks around 430 nm, and these spectral patterns were the same as those of the $Tp^{iPr_2,X}$ analogues of 4^X , $[Ni^{II}(O_2CC_6H_4Cl)(Tp^{iPr_2,X})]$ (4^X). In mass spectra of the product derived from CH_2Cl_2 solution, no peak of the chloride complexes 3^X existed, whereas peaks consistent with the formula as $[4^X + O]$ ($m/z = 933$) were observed. 1H NMR spectra of the product mixture showed the existence of 4^X and another species, of which the three-fold symmetry of the tris(pyrazolyl)borate ligand moiety was lost. Moreover, the 1H NMR spectrum derived from 2^{Br} contained a signal at 16.5 ppm, of which the proton was exchangeable with external D_2O . These spectral features suggest the progress of partial oxygenation of the methine portion of the isopropyl groups of $Tp^{iPr_2,X}$ proximal to the nickel center, and the resultants were tentatively assigned as nickel(II)-carboxylate complexes with hydroxylated $Tp^{iPr_2,X}$ ligands, $[Ni^{II}(O_2CC_6H_4Cl)\{HB(3-Me_2C(OH)-5-iPrpz)(3,5-iPr_2pz)_2\}]$ (5^X ; see Scheme 1). Such intra-molecular ligand oxygenations have been observed in various transition metal-active oxygen complexes such as $M_2(\mu-O)_2$ and $M-OOR$, including the nickel- and cobalt- Tp^{iPr_2} complexes.^{7,8d,8e,13,24} Interestingly, the selectivity for the

ligand-hydroxylated compounds 5^X seems to be correlated with the nature of X on [View Article Online](#) $Tp^{iPr2,X}$. The products ratio $5^X:4^X$ were 7:1 from 2^{Br} and 1:2 from 2^H , respectively (determined by 1H NMR). Although the hindered $Tp^{iPr2,X}$ complexes cannot catalyze cyclohexane hydroxylation, the higher selectivity toward the intra-molecular alkyl group hydroxylation on 2^{Br} is consistent with the alcohol selectivity of the $Tp^{Me2,Br}$ ligand catalyst being higher than that of the non-brominated Tp^{Me2} ligand catalyst.

Kinetics of the thermal decomposition process of 2^X

In the absence of external substrate, both 2^X and 2^{Br} decomposed spontaneously in accord with first-order kinetics. The bromine-containing ligand complexes are more stable than the parent non-brominated complex. Also, 2^{Br} is more stable than 2^{Br} (Table 5). These orders illustrate that how the electronic and steric natures of the ligands affect the lifetime of the acylperoxo species and the substrate-oxidizing activities. The bulky alkyl groups (i.e. 3-*i*Pr on $Tp^{iPr2,X}$) wrap the O–O moiety of the metal-bound acylperoxide to stabilize 2^X but hinder the reaction with external substrate. The smaller methyl substituents on $Tp^{Me2,X}$ are an appropriate size to provide substrates-accessible space allowing for the catalyses of 2^X . As well as the previously reported nickel(II)-alkylperoxo complexes with $Tp^{iPr2,X}$,¹³ incorporation of the electron-withdrawing bromine at the distal fourth position of the pyrazolyl groups in $Tp^{R2,X}$ results in increases in the stability of the nickel(II)-acylperoxo species.

[Table 5]

Interestingly, kinetic isotope effects were observed during the decay of 2^X in CH_2Cl_2/CD_2Cl_2 . The observed k_H/k_D values at 253 K were 2.5 for 2^H and 3.2 for 2^{Br} , respectively. Interestingly, the yields of the chloride complexes 3^X decreased when the deuterated solvent was used (3^H : 51 % in $CH_2Cl_2 \rightarrow$ 12 % in CD_2Cl_2 at $-20^\circ C$, 3^{Br} : 36 % in $CH_2Cl_2 \rightarrow$ 7 % in CD_2Cl_2 at $0^\circ C$). Moreover, the decomposition of 2^{Br} in CD_2Cl_2 led to oxygenation of the methyl group of $Tp^{Me2,Br}$ (Fig. S9). These findings indicate an interaction between the solvent molecule and 2^X , and hydrogen atom

abstraction from the solvent may occur concomitant with O–O bond rupture of 2^{X} .²⁵ [View Article Online](#)

The large negative values of an activation entropy for the self decomposition of 2^{X} in CH_2Cl_2 (Fig. S11 and Table S5) indicate the reaction proceeds through an associative transition state, and that is consistent with the interaction between the solvent molecule and 2^{X} . The observed KIE values are, however, not so large even at low temperatures. Upon the decomposition of 2^{Br} (2.0 mM) in the mixture ($v/v = 1/1$) of CD_2Cl_2 and C_6H_{12} or C_6D_{12} at 273 K, the observed KIE was 1.6 ($k(\text{CD}_2\text{Cl}_2/\text{C}_6\text{H}_{12})$ and $k(\text{CD}_2\text{Cl}_2/\text{C}_6\text{D}_{12})$ were $5.2 \times 10^{-4} \text{ s}^{-1}$ and $3.3 \times 10^{-4} \text{ s}^{-1}$, respectively). However, high concentration of cyclohexane ($v/v = 1/20$ of CD_2Cl_2 and C_6H_{12} or C_6D_{12}) led to negligible KIE value (decomposition rate of 2 mM of 2^{Br} at 283 K were $k(\text{CD}_2\text{Cl}_2/\text{C}_6\text{H}_{12}) = 2.8 \times 10^{-3} \text{ s}^{-1}$ and $k(\text{CD}_2\text{Cl}_2/\text{C}_6\text{D}_{12}) = 2.5 \times 10^{-3} \text{ s}^{-1}$). Therefore, 2^{X} themselves have the ability of hydrogen atom abstraction from aliphatic C–H group,²⁶ but a putative nickel–oxygen species such as $\text{Ni}^{\text{III}}=\text{O}$ or $\text{Ni}^{\text{II}}-\text{O}\cdot$ resulting from the O–O homolysis of 2^{X} may work as a major oxidant on catalytic cyclohexane hydroxylation (Scheme 2). Recently, the hydrogen atom abstraction ability of the mononuclear nickel(III)-oxo species, which is generated from the reaction of $[\text{Ni}^{\text{II}}(\text{OTf})(\text{TMG}_3\text{tren})]^+$ (TMG₃tren denotes tris[2-(N-tetramethylguanidyl)ethyl]amine) with 1 equiv. of *m*CPBA, has been reported.⁶ In the $\text{Tp}^{\text{R}2,\text{X}}\text{Ni}$ systems, however, we could not identify any intermediates during decomposition of the nickel(II)-acylperoxo species 2^{X} by spectroscopy (UV/Vis and EPR), and there is no direct evidence for the contribution of the nickel(III)-oxo and related species.²⁷

[Scheme 2]

Conclusion

The nickel complexes with $\text{Tp}^{\text{Me}2,\text{X}}$ exhibit alkane hydroxylation catalyses with *m*CPBA oxidant. Introduction of electron-withdrawing group (= EWG) on the pyrazolyl backbone of $\text{Tp}^{\text{Me}2,\text{X}}$ leads to increases in the alcohol selectivity. Effectiveness of the introduction of EWG on the metal supporting ligand for the selective hydroxylation of

alkanes has been demonstrated on iron-heme compounds.²⁸ An electrophilicity of the active oxidant may be enhanced by EWG-containing ligand, and our results indicate that the common concept for the ligand design, that is the fine tuning of the electronic property without changing the structure of the metal-supporting scaffold, is applicable to non-heme catalysts. The thermal stability of the nickel(II)-*m*CPBA species is also enhanced by the EWG-containing ligands Tp^{R²,Br}, which might weaken the ability of back-donation from the metal center to the σ^* orbital of the peroxide moiety.^{13,29} Kinetic and product analyses of the decomposition of the nickel(II)-*m*CPBA complexes suggest that the nickel(II)-acylperoxo complex, Ni^{II}-OOC(=O)C₆H₄-*meta*-Cl, is an alternative oxidant. However, hydrogen atom abstracting potential of nickel(II)-*m*CPBA complexes with Tp^{Me²,Br} is not so high and the previously proposed O–O bond cleaved species (i.e. Ni^{II}-O• or Ni^{III}=O) may be a major active oxidant for the catalytic cyclohexane oxygenation.

Experimental Section

General

All manipulations were performed under argon by standard Schlenk techniques. THF, Et₂O, pentane, toluene, CH₂Cl₂, MeCN were purified over a Glass Contour Solvent Dispensing System under Ar atmosphere. CF₃C₆H₅ was distilled using sodium as a drying agent and then stored under argon. *meta*-Chloroperbenzoic acid (= *m*CPBA) was washed with KH₂PO₄-NaOH buffer solution (pH 7.4) and pure water in order to remove *meta*-chlorobenzoic acid. Other reagents of the highest grade commercially available were used without further purification. The catalyst precursors [(Ni^{II}Tp^{R²,X})₂(μ -OH)₂] (**1**^X (R = Me) and **1**'^X (R = *i*Pr); X = H, Br) and their starting materials were prepared by the methods described in the literature.^{8e,13,14,30} Elemental analyses were performed on a Perkin-Elmer CHNS/O Analyzer 2400II. IR measurements of KBr pellets of solid compounds were carried out by using JASCO FT/IR-5300 or FT/IR 4200 spectrometers. IR spectra of the *in situ*-generated solution

samples were recorded using a Mettler Toledo ReactIR iC10. NMR spectra were recorded on Bruker AC-200 (^1H , 200.0 MHz) or JEOL ECA-500 (^1H , 500.0 MHz) spectrometers. Chemical shifts (δ) were reported in ppm downfield from internal SiMe_4 . UV/Vis spectra were recorded on JASCO V-570, V650 or Agilent 8453 spectrometers equipped with a UNISOKU CoolSpeK USP-203-A for low-temperature measurements. Mass spectra were measured on a JEOL JMS-700 by a field desorption (FD) ionization method or a JEOL JMS-T100LC by an electrospray ionization (ESI) method. Gas chromatographic (GC) analyses were carried out on a Shimadzu GC-2010 instrument with a flame ionization detector equipped with a RESTEK Rtx-1701 (30 m, 0.25 mmID, 0.25 μm df) capillary column. GC-MS analyses were carried out on a Shimadzu PARVUM2 system equipped with a RESTEK Rtx-5MS (30 m, 0.25 mmID, 0.25 μm df) capillary column.

Catalytic cyclohexane oxidation with *m*CPBA

All reactions were carried at 313 K under Ar, and the products were analyzed by GC and GC-MS with an internal standard. Cyclohexane (0.28 mL, 2.6 mmol) was added to a 5.2 mM $\text{CF}_3\text{C}_6\text{H}_5$ solution of $\mathbf{1}^{\text{X}}$ or $\mathbf{1}^{\text{H}}$ (5.0 mL, 26 μmol). Next, 45 mg of *m*CPBA (260 μmol) was added to this solution with stirring. The reactions with large excess substrate were carried out as follows. Due to the insolubility of the catalyst precursors ($\mathbf{1}^{\text{X}}$ and $\mathbf{1}^{\text{H}}$) and *m*CPBA toward cyclohexane, a minimal amount of CH_2Cl_2 was used as solvent: 1.0 mL of a 2.6 mM CH_2Cl_2 solution of $\mathbf{1}^{\text{X}}$ or $\mathbf{1}^{\text{H}}$ (2.6 μmol) was added to 1.4 mL of cyclohexane (13 mmol) under Ar. Then 45 mg of *m*CPBA (260 μmol) was added.

Synthesis of the nickel(II)-*m*CPBA complexes

$[\text{Ni}^{\text{II}}(\text{OOC}(=\text{O})\text{C}_6\text{H}_4\text{Cl})(\text{Tp}^{i\text{Pr}2,\text{Br}})] (\mathbf{2}^{\text{Br}})$. The synthetic procedure for the isolable $\text{Tp}^{i\text{Pr}2,\text{Br}}$ complex $\mathbf{2}^{\text{Br}}$ is described as a typical example. The hydroxo complex $\mathbf{1}^{\text{Br}}$ (250 mg, 0.16 mmol) was dissolved in Et_2O (15 mL), and the solution was

cooled at 233 K. Then 5 mL of an Et₂O solution of *m*CPBA (58.2 mg, 0.33 mmol) was added to the cold solution of **2**^{Br}. The resulting pale blue solution was stirred for 10 min at 233 K, and the solvent was then concentrated by evaporation while maintaining a low temperature. Refrigeration of the concentrated solution at 195 K yielded the pale blue powder of **2**^{Br}. Almost quantitative oxygenation of Ph₃P to Ph₃P=O (97 % yield based on **2**^{Br} analyzed by ³¹P NMR) in Et₂O at 293 K (7 equiv. of Ph₃P was applied) indicated the isolated blue powder compound was a pure acylperoxo complex. UV/Vis (Et₂O, 233 K): λ(ε)=386 (151), 654 nm (50); IR (KBr): ν=2586 (BH), 1637 cm⁻¹ (CO).

The other ligand complexes **2**^X and **2**^H could be generated by similar procedures, and spectroscopic characterization by UV/Vis and IR were performed without isolation.

Products analyses of the spontaneous decomposition of the nickel(II)-*m*CPBA complexes

The product complexes derived from the spontaneous decomposition of **2**^X and **2**^X were characterized by comparison with the UV-vis spectral data of the nickel(II)-chloride and *meta*-chlorobenzoate complexes **3**^X, **3**^X, **4**^X, and **4**^X. Except for the previously reported chlorido complexes with Tp^{Me2} (**3**^H),²³ Tp^{iPr2} (**3**^H),¹⁴ and Tp^{iPr2,Br} (**3**^{Br}),¹³ the authentic complexes were synthesized as follows.

[Ni^{II}(Cl)(Tp^{Me2,Br})] (**3**^{Br}). THF solution (20 mL) of NaTp^{Me2,Br} (1.00 g, 1.80 mmol) was slowly added to a methanol solution (20 mL) of NiCl₂·6H₂O (0.854g 3.6 mmol) over 30 min at RT. The green solution was stirred for 30 min, and the solvent was then evaporated. The green residue was re-dissolved into 100 mL of CH₂Cl₂, and the insoluble green powder was removed by filtration through a celite pad, after which a reddish filtrate was evaporated to dryness to give a green solid. The solid was re-dissolved into 100 mL of MeCN, and the insoluble purple residue was removed by filtration through a celite pad to give a bluish-green filtrate. Evaporation of the solution gave a green solid. Crystallization from toluene gave the title complex as a green platelet crystal (0.498 g, 0.74 mmol, 41%). UV/Vis (CH₂Cl₂): λ(ε)=481 (360), 801

(105), 900 nm (120); IR (KBr): $\nu=2532\text{ cm}^{-1}$ (BH); $^1\text{H NMR}$ (500 MHz, CD_2Cl_2 , r.t.): $\delta=-13.16$ (2H, BH), -8.52 (18H, Me), 3.74 ppm (18H, Me); elemental analysis: calcd (%) for $\text{C}_{18.5}\text{H}_{23}\text{N}_6\text{BBBr}_3\text{ClNi}$ ($\mathbf{3}^{\text{Br}} \cdot 1/2\text{toluene}$): C 32.96, H 3.44, N 12.47; found: C 33.48, H 3.23, N 12.65. The molecular structure was determined by X-ray crystallography, and the details are provided as Supporting information.

$[\text{Ni}^{\text{II}}(\text{O}_2\text{CC}_6\text{H}_4\text{Cl})(\text{Tp}^{\text{R}2,\text{Br}})]$ ($\mathbf{4}^{\text{X}}$ and $\mathbf{4}'^{\text{X}}$). As a typical example, the synthetic procedure for $[\text{Ni}^{\text{II}}(\text{O}_2\text{CC}_6\text{H}_4\text{Cl})(\text{Tp}^{\text{Me}2,\text{Br}})]$ ($\mathbf{4}^{\text{Br}}$) is described. The hydroxo complex $\mathbf{1}^{\text{Br}}$ (122 mg, 0.10 mmol) and *meta*-chlorobenzoic acid (*mCBA*, 34.4 mg, 0.22 mmol) were dissolved in 10 mL of CH_2Cl_2 . The green solution was stirred for 30 min at ambient temperature, and the solvent was then evaporated. The green residue was recrystallized from slow evaporation of EtOH to give an ethanol adduct of $\mathbf{4}^{\text{Br}}$, $[\text{Ni}^{\text{II}}(\text{O}_2\text{CC}_6\text{H}_4\text{Cl})(\text{Tp}^{\text{Me}2,\text{Br}})(\text{C}_2\text{H}_5\text{OH})_2]$, as green block crystal (127 mg, 0.15 mmol, 75 % yield). UV/Vis (CH_2Cl_2): $\lambda(\epsilon)=421$ (210), 682 (47), 843 nm (39); (toluene): $\lambda(\epsilon)=421$ (180), 685 (38), 851 nm (31); IR (KBr): $\nu=2544$ (BH), 1591 cm^{-1} (COO); $^1\text{H NMR}$ (500 MHz, CD_2Cl_2 , r.t.): $\delta=-10.51$ (1H, BH), -9.45 (9H, Me), 0.62 (9H, Me), 2.36 (6H; EtOH), 4.28 (4H; EtOH) 6.06 (1H; *mCBA*), 9.39 (1H; *mCBA*), 11.04 (1H; *mCBA*), 11.47 ppm (1H; *mCBA*); elemental analysis: calcd (%) for $\text{C}_{26}\text{H}_{35}\text{BBBr}_3\text{ClNiO}_4$ ($\mathbf{4}^{\text{Br}} \cdot 2\text{EtOH}$): C 37.16, H 4.20, N 10.00; found: C 37.25, H 3.98, N 10.11.

The other nickel(II)-*mCBA* complexes were synthesized by the same procedure.

$[\text{Ni}^{\text{II}}(\text{O}_2\text{CC}_6\text{H}_4\text{Cl})(\text{Tp}^{\text{Me}2})]$ ($\mathbf{4}^{\text{H}}$). The $\text{Tp}^{\text{Me}2}$ complex $\mathbf{4}^{\text{H}}$ is synthesized by the reaction of $\mathbf{1}^{\text{H}}$ (111 mg, 0.15 mmol) and *mCBA* (51.6 mg, 0.33 mmol) in THF. Recrystallization from MeCN yielded the yellow-green solid of $\mathbf{4}^{\text{H}}$ (60.1 mg, 0.12 mmol, 40 % yield). UV/Vis (toluene): $\lambda(\epsilon)=428$ (213), 686 nm (61); IR (KBr): $\nu=2514$ (BH), 1591 cm^{-1} (COO); elemental analysis: calcd(%) for $\text{C}_{22}\text{H}_{26}\text{N}_6\text{BClNiO}_2$ ($\mathbf{4}^{\text{H}}$): C 51.67, H 5.12, N 16.43; found C 51.20, H 4.95, N 16.47.

$[\text{Ni}^{\text{II}}(\text{O}_2\text{CC}_6\text{H}_4\text{Cl})(\text{Tp}^{\text{iPr}2})]$ ($\mathbf{4}^{\text{H}}$). The hydroxonickel complex with $\text{Tp}^{\text{iPr}2}$ $\mathbf{1}^{\text{H}}$ (75.6 mg, 0.0698 mmol) and *mCBA* (21.8 mg, 0.139 mmol) were stirred in 15 mL of

Et₂O for 10 min at room temperature. After removal of the volatiles under vacuum, the resulting yellow-green solid of **4^H** was recrystallized from pentane (76.5 mg, 0.113 mmol, 81% yield). UV/Vis (CH₂Cl₂): $\lambda(\epsilon)$ =429 (250), 690 (59), 854 nm (47); IR (KBr): ν =2549 cm⁻¹ (BH); ¹H NMR (200 MHz, C₆D₆, r.t.): δ =-3.6 (3H, br, CH of *i*Pr), 0.07 (18H, s, Me of *i*Pr), 2.61 (21H, s, Me and CH of *i*Pr), 4.80, 9.04, 11.1, 11.5 (1H×4, s×4, Ph of *m*CBA), 75.4 ppm (3H, s, pz-4H); MS (FD): m/z =679 ([**4^H**]⁺); elemental analysis: calcd (%) for C₃₄H₅₀N₆BClNiO₂ (**4^H**): C 60.08, H 7.41, N 12.36; found: C 59.86, H 7.43, N 12.43.

[Ni^{II}(O₂CC₆H₄Cl)(Tp^{*i*Pr₂,Br})] (**4^{Br}**). Recrystallization of the reaction mixture of **1^{Br}** (352 mg, 0.226 mmol) and two equiv. of *m*CBA (70.8 mg, 0.452 mmol) from hexane yielded the yellow-green powder of the Tp^{*i*Pr₂,Br} analogue **4^{Br}** (217 mg, 0.120 mmol, 53% yield). UV/Vis (Et₂O): $\lambda(\epsilon)$ =416 (240), 694 nm (52); IR (KBr): ν =2578 cm⁻¹ (BH); ¹H NMR (200 MHz, C₆D₆, r.t.): δ =-11.1 (1H, BH), -0.75 (br, CH of *i*Pr), 1.78 (18H, s, Me of *i*Pr), 2.12 (21H, br, Me and CH of *i*Pr), 5.10, 9.10 (1H×2, s×2, Ph of *m*CBA), 13.1 ppm (2H, br, Ph of *m*CBA); MS (FD): m/z =917 ([**4^{Br}**]⁺); elemental analysis: calcd (%) for C₃₄H₄₇N₆BBR₃ClNiO₂ (**4^{Br}**): C 44.56, H 5.17, N 9.17; found: C 44.85, H 5.40, N 8.89.

The molecular structures of an EtOH adduct of **4^{Br}** and **4^H** were determined by X-ray crystallography, and the details are provided as Supporting information.

Acknowledgements

This work was supported in part by a Grant in-Aid for Scientific Research (Nos. 20037063 and 20360367), a Cooperative Research Program of “Network Joint Research Center for Materials and Devices (Nos. 2011169 and 2012216)”, a Scientific Frontier Research Project, and a Strategic Development of Research Infrastructure for Private Universities from the Ministry of Education, Culture, Sports, Science, and Technology (MEXT), Japan. S. H. and J. N. also thank Kanagawa University for financial support.

References

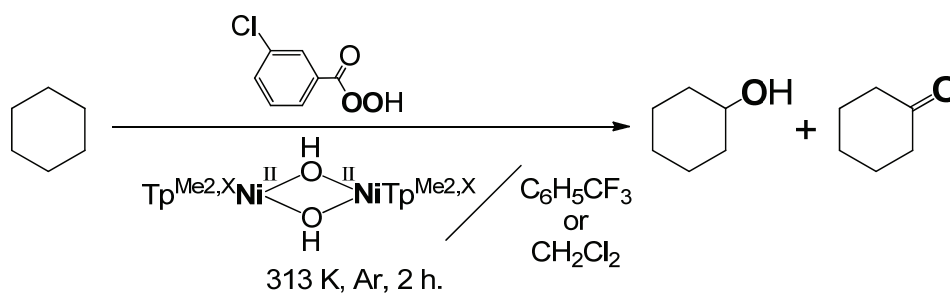
[View Article Online](#)

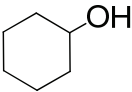
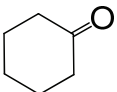
- 1 *Metal-Catalyzed Oxidations of Organic Compounds* (Eds.: R. A. Sheldon and J. K. Kochi), Academic Press, New York, 1981.
- 2 M. Costas, K. Chen and L. Que, Jr., *Coord. Chem. Rev.*, 2000, **200** – **202**, 517 – 544.
- 3 G. A. Russell, *J. Am. Chem. Soc.*, 1957, **79**, 3871 – 3877.
- 4 Reviews for example: (a) *Biomimetic Oxidations Catalyzed by Transition Metal Complexes* (Ed.: B. Meunier), Imperial College Press, London, 2000; (b) Thematic issue: *Homogeneous Biomimetic Oxidation Catalysis* (Eds.: R. V. Eldik and J. Reedijk), *Adv. Inorg. Chem.*, 2006, **58**, 1 – 290; (c) *Metal-Oxo and Metal-Peroxo Species in Catalytic Oxidations* (Ed.: B. Meunier), *Struct. Bonding*, 2000, **97**, 1 – 303; (d) L. Que, Jr. and W. B. Tolman, *Nature*, 2008, **455**, 333 – 340.
- 5 Alkane hydroxylation with *m*CPBA catalyzed by nickel complexes with tetradentate ligands: (a) T. Nagataki, Y. Tachi and S. Itoh, *Chem. Commun.*, 2006, 4016 – 4018; (b) T. Nagataki, K. Ishii, Y. Tachi and S. Itoh, *Dalton Trans.*, 2007, 1120 – 1128; (c) T. Nagataki and S. Itoh, *Chem Lett.*, 2007, **36**, 748 – 749; (d) M. Balamurugan, R. Mayilmurugan, E. Sureshb and M. Palaniandavar, *Dalton Trans.*, 2011, **40**, 9413 – 9424.
- 6 F. F. Pfaff, F. Heims, S. Kundu, S. Mebs and K. Ray, *Chem. Commun.*, 2012, **48**, 3730 – 3732.
- 7 S. Hikichi, H. Okuda, Y. Ohzu and M. Akita, *Angew. Chem. Int. Ed.*, 2009, **48**, 188 – 191.
- 8 Intramolecular C–H oxygenation mediated by nickel complexes of active oxygen species: (a) D. Chen and A. E. Martell, *J. Am. Chem. Soc.*, 1990, **112**, 9411 – 9412; (b) D. Chen, R. J. Motekaitis and A. E. Martell, *Inorg. Chem.*, 1991, **30**, 1396 – 1402; (c) E. Kimura, R. Machida and M. Kodama, *J. Biol. Inorg. Chem.*, 1997, **2**, 74 – 82; (d) S. Hikichi, M. Yoshizawa, Y. Sasakura, H.

- Komatsuzaki, M. Akita and Y. Moro-oka, *Chem. Lett.*, 1999, 979 – 980; (e) S. Hikichi, M. Yoshizawa, Y. Sasakura, H. Komatsuzaki, Y. Moro-oka and M. Akita, *Chem.–Eur. J.*, 2001, **7**, 5011 – 5028; (f) S. Itoh, H. Bandoh, S. Nagatomo, T. Kitagawa and S. Fukuzumi, *J. Am. Chem. Soc.*, 1999, **121**, 8945 – 8946; (g) S. Itoh, H. Bandoh, M. Nakagawa, S. Nagatomo, T. Kitagawa, K. D. Karlin and S. Fukuzumi, *J. Am. Chem. Soc.*, 2001, **123**, 11168 – 11178; (h) A. Kunishita, Y. Doi, M. Kubo, T. Ogura, H. Sugimoto and S. Itoh, *Inorg. Chem.*, 2009, **48**, 4997 – 5004; (i) T. Tano, Y. Doi, M. Inosako, A. Kunishita, M. Kubo, H. Ishimaru, T. Ogura, H. Sugimoto and S. Itoh, *Bull. Chem. Soc. Jpn.*, 2010, **83**, 530 – 538; (j) J. Cho, H. Furutachi, S. Fujinami and M. Suzuki, *Angew. Chem, Int. Ed.*, 2004, **43**, 3300 – 3303; (k) J. Cho, H. Furutachi, S. Fujinami, T. Tosha, H. Ohtsu, O. Ikeda, A. Suzuki, M. Nomura, T. Uruga, H. Tanida, T. Kawai, K. Tanaka, T. Kitagawa and M. Suzuki, *Inorg. Chem.*, 2006, **45**, 2873 – 2885; (l) M. Suzuki, *Acc. Chem. Res.*, 2007, **40**, 609 – 617; (m) K. Honda, J. Cho, T. Matsumoto, J. Roh, H. Furutachi, T. Tosha, M. Kubo, S. Fujinami, T. Ogura, T. Kitagawa and M. Suzuki, *Angew. Chem. Int. Ed.*, 2009, **48**, 3304 – 3307; (n) A. Company, S. Yao, K. Ray and M. Driess, *Chem.–Eur. J.*, 2010, **16**, 9669 – 9675; (o) S. Yao, C. Herwig, Y. Xiong, A. Company, E. Bill, C. Limberg and M. Driess, *Angew. Chem. Int. Ed.*, 2010, **49**, 7054 – 7058; (p) S. Yao and M. Driess, *Acc. Chem. Res.*, 2012, **45**, 276 – 287.
- 9 D. Schröder and H. Schwarz, *Angew. Chem. Int. Ed. Engl.*, 1995, **34**, 1973 – 1995.
- 10 Y. Shiota and K. Yoshizawa, *J. Am. Chem. Soc.*, 2000, **122**, 12317 – 12326.
- 11 A. W. Pierpont and T. R. Cundari, *Inorg. Chem.*, 2010, **49**, 2038 – 2046.
- 12 (a) S. Trofimenko, *Scorpionates – The Coordination Chemistry of Polypyrazolylborate Ligands*, Imperial College Press, London, 1999; (b) C. Pettinari, *Scorpionates II: Chelating Borate Ligands*, Imperial College Press, London, 2008.

- 13 S. Hikichi, C. Kobayashi, M. Yoshizawa and M. Akita, *Chem.–Asian J.*, 2010, **5**, 2086 – 2092. [View Article Online](#)
- 14 N. Kitajima, S. Hikichi, M. Tanaka and Y. Moro-oka, *J. Am. Chem. Soc.*, 1993, **115**, 5496 – 5508.
- 15 W. Nam, J. Y. Ryu, I. Kim and C. Kim, *Tetrahedron Lett.*, 2002, **43**, 5487 – 5490.
- 16 W. Nam, I. Kim, Y. Kim and C. Kim, *Chem. Commun.*, 2001, 1262 – 1263.
- 17 K. Kamata, K. Yonehara, Y. Nakagawa, K. Uehara and N. Mizuno, *Nature Chem.*, 2010, **2**, 478 – 483.
- 18 (a) W. Nam, M. H. Lim, S. K. Moon and C. Kim, *J. Am. Chem. Soc.*, 2000, **122**, 10805 – 10809; (b) A.-R. Han, Y. J. Jeong, Y. Kang, J. Y. Lee, M. S. Seo and W. Nam, *Chem. Commun.*, 2008, 1076 – 1078.
- 19 If the nickel(II) centers of $\mathbf{1}^X$ was oxidized to nickel(III) by *m*CPBA at initial step and following ligand exchange reaction led to nickel-acylperoxo complexes, total ratio of Ni to *m*CPBA would be 1:1.5 or more as found for the non-heme iron(II) complex. K. Ray, S. M. Lee and L. Que, Jr., *Inorg. Chim. Acta*, 2008, **361**, 1066 – 1069.
- 20 J. T. Groves and Y. Watanabe, *Inorg. Chem.*, 1987, **26**, 785 – 786.
- 21 P. Ghosh, Z. Tyeklar, K. D. Karlin, R. R. Jacobson and J. Zubieta, *J. Am. Chem. Soc.*, 1987, **109**, 6889 – 6891.
- 22 N. Kitajima, K. Fujisawa and Y. Moro-oka, *Inorg. Chem.*, 1990, **29**, 357 – 358.
- 23 P. J. Desrochers, J. Telsler, S. A. Zvyagin, A. Ozarowski, J. Krzystek and D. A. Vicic, *Inorg. Chem.*, 2006, **45**, 8930 – 8941.
- 24 S. Hikichi, H. Komatsuzaki, M. Akita and Y. Moro-oka, *J. Am. Chem. Soc.*, 1998, **120**, 4699 – 4710.
- 25 On the basis of the observation of KIE upon the thermal decomposition of the copper(II)-alkylperoxo complex in the deuterated solvent (CD_3CN), concerted O–O fission and H abstraction are proposed: T. Tano, M. Z. Ertem, S.

- Yamaguchi, A. Kunishita, H. Sugimoto, N. Fujieda, T. Ogura, C. J. Cramer and S. Itoh, *Dalton Trans.*, 2011, **40**, 10326 – 10336. [View Article Online](#)
- 26 In the heme-Fe/*m*CPBA system, both (por)Fe^{III}-acylperoxo and (por•)Fe^{IV}=O (por• denotes 1e⁻ oxidized porphyrinate ligand) are proposed as active oxidants for alkane hydroxylation. See ref. 18(a).
- 27 Existence of nickel(IV)-oxo species, which would generate via O–O heterolysis of the nickel(II)-acylperoxo species or intramolecular electron transfer from the nickel center of the to weakly binding carboxyl radical in the nickel(III)-oxo species (O–O homolysis intermediate in Scheme 2) cannot be excluded, although any nickel(IV) complexes with Tp^R have not been reported so far.
- 28 (a) W. Nam, *Acc. Chem. Res.*, 2007, **40**, 522 – 531; (b) D. Dolphin, T. G. Traylor and L. Y. Xie, *Acc. Chem. Res.*, 1997, **30**, 251 – 259.
- 29 Stabilization of Cu₂(μ-η²:η²-O₂) species by Tp^{CF₃,Me} has been reported. (a) Z. Hu, R. D. Williams, D. Tran, T. G. Spiro and S. M. Gorun, *J. Am. Chem. Soc.*, 2000, **122**, 3556 – 3557; (b) Z. Hu, G. N. George and S. M. Gorun, *Inorg. Chem.*, 2001, **40**, 4812 – 4813; (c) G. Aullón, S. M. Gorun and S. Alvarez, *Inorg. Chem.*, 2006, **45**, 3594 – 3601.
- 30 S. Hikichi, Y. Sasakura, M. Yoshizawa, Y. Ohzu, Y. Moro-oka and M. Akita, *Bull. Chem. Soc. Jpn.*, 2002, **75**, 1255 – 1262.

Table 1 Catalytic activity of **1^H** for cyclohexane oxidation[View Article Online](#)

Entry	Complex	Products / μmol^a		A/K ^b	TON ^c
					
Solvent: $\text{C}_6\text{H}_5\text{CF}_3$ (5 mL), Amount of 1^X = 26 μmol , Ni: <i>m</i> CPBA: C_6H_{12} = 1:5:50					
1	1^H	10.7	6.4	1.7	0.5
2	1^{Br}	35.9	20.4	1.8	1.5
Solvent: CH_2Cl_2 (1 mL), Amount of 1^X = 13 μmol , Ni: <i>m</i> CPBA: C_6H_{12} = 1:50:2500					
3	1^H	227	7.0	32	46
4	1^{Br}	210	4.0	53	42

^a ϵ -Caprolactone, which would form through the reaction of cyclohexanone and *m*CPBA, was not obtained under the examined reaction conditions. ^b A/K = yield of cyclohexanol / yield of cyclohexanone. ^c TON = (cyclohexanol + 2 × cyclohexanone)/nickel.

Table 2 Catalytic methylcyclohexane oxidation by **1^X** with *m*CPBA

Entry	Complex	Products / μmol ^a						TON ^c
		3°-ol	2°-ol	2°-one	3°-ol: 2°-ol ^b	TON ^c		
1	1^H	47.1	61.6 ^b	3.8	0.6	0.9	35 : 65	43
2	1^{Br}	45.6	62.4 ^b	3.3	0.5	0.8	34 : 66	42
3	none	0.9	0.9 ^b	0	0	0	77 : 23	2 ^d
4	none ^e	153.6	10.4	1.9	0.5	0.2	84 : 16	36 ^d

^a ε-Caprolactones, which would be formed through the reaction of methylcyclohexanones and *m*CPBA, and cyclohexanecarboxaldehyde, which would be formed by oxidation of cyclohexanemethanol (= 1°-ol), were not obtained under the examined reaction conditions. ^b A small amount of 2-methylcyclohexanone was included. ^c TON = (3°-ol + 2°-ol + 1°-ol + 2×2°-one)/nickel. ^d Values based on 5.2 μmol of virtual nickel catalyst. ^e Reaction conditions: 353 K, without CH₂Cl₂, 2 h.

View Article Online

Table 3 UV/Vis spectral data of 2^X and $2'^X$ ^a[View Article Online](#)

	2^H ^b	2^{Br} ^b	$2'^H$ ^c	$2'^{Br}$ ^c
λ [nm]	386 (148)	382 (108)	386 (260)	386 (151)
$(\epsilon$ [$M^{-1} \text{ cm}^{-1}$])	633 (42)	628 (22)	654 (68)	654 (50)

^a ϵ values of 2^X and $2'^H$ were estimated based on the concentration of nickel in the parent hydroxo complexes 1^X and $1'^H$, while the ϵ of $2'^{Br}$ was determined based on the used $2'^{Br}$, which was isolated as a pale blue powder by refrigeration. ^b CH_2Cl_2 solution at 223 K. ^c Et_2O solution at 233 K.

Table 4 IR band of $\nu_{\text{C=O}}$ of the acyl component^a[View Article Online](#)

Compound	$\nu_{\text{C=O}}$ [cm^{-1}]	Ref.
2^H	1646 ^a	This work
2^{Br}	1661, 1643 ^{a, c}	This work
2',^H	1643 ^b	This work
2',^{Br}	1637 ^b	This work
[Fe ^{III} (OOC(=O)C ₆ H ₄ Cl) (TTPPP)]	1744 ^b	20
[Cu ^{II} ₂ (XYL-O-)(μ -OOC(=O)C ₆ H ₄ Cl)] ²⁺	1745 ^b	21
[Cu ^{II} (OOC(=O)C ₆ H ₄ Cl)(Tp ^{iPr2})]	1640 ^b	22
<i>m</i> CPBA	1738 ^a , 1726 ^b	This work ^d
<i>m</i> CBA	1706 ^a , 1696 ^b	This work ^d

^a CH₂Cl₂ solution. ^b Solid sample (KBr or Nujol). ^c Two peaks appeared. See supporting information (Figure S6). ^d Measured under the same conditions for **2^X** (CH₂Cl₂ solution at 223 K) and for **2',^X** (KBr pellet at room temperature).

Table 5 First order rate for the decomposition of 2^X and $2'^X$ [View Article Online](#)

solvent (Temp.)	rate / s ⁻¹			
	2^H	2^{Br}	$2'^H$	$2'^{Br}$
CH ₂ Cl ₂ (273K)	4.2×10^{-3}	1.7×10^{-3}	— ^a	— ^a
CH ₂ Cl ₂ (253K)	8.8×10^{-4}	1.6×10^{-4}	— ^a	— ^a
CD ₂ Cl ₂ (253K)	3.5×10^{-4}	5.0×10^{-5}	— ^a	— ^a
Toluene (273 K)	3.8×10^{-3}	2.3×10^{-3}	— ^a	9.7×10^{-4}
Et ₂ O (273 K)	— ^a	— ^a	2.5×10^{-3}	5.1×10^{-4}

^a not measured.

List of the Legends of Schemes and Figures

[View Article Online](#)

Scheme 1 Formation of the nickel(II)-acylperoxo complexes and their thermal decomposition products.

Scheme 2 Possible reaction pathways for the thermolysis of 2^X .

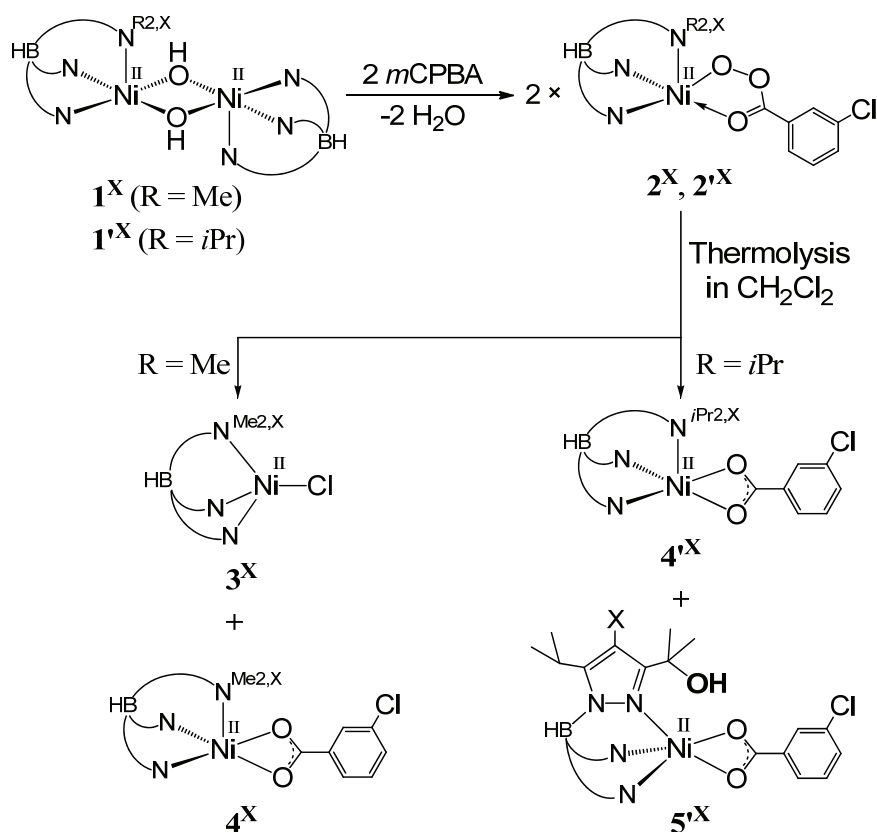
Fig. 1 Cyclohexane oxygenation by the Ni/*m*CPBA system and the ligands used as the support for nickel.

Fig. 2 Time course of cyclohexane oxidation with *m*CPBA mediated by 1^X under a large excess of substrate (corresponding to the entries 3 and 4 in Table 1).

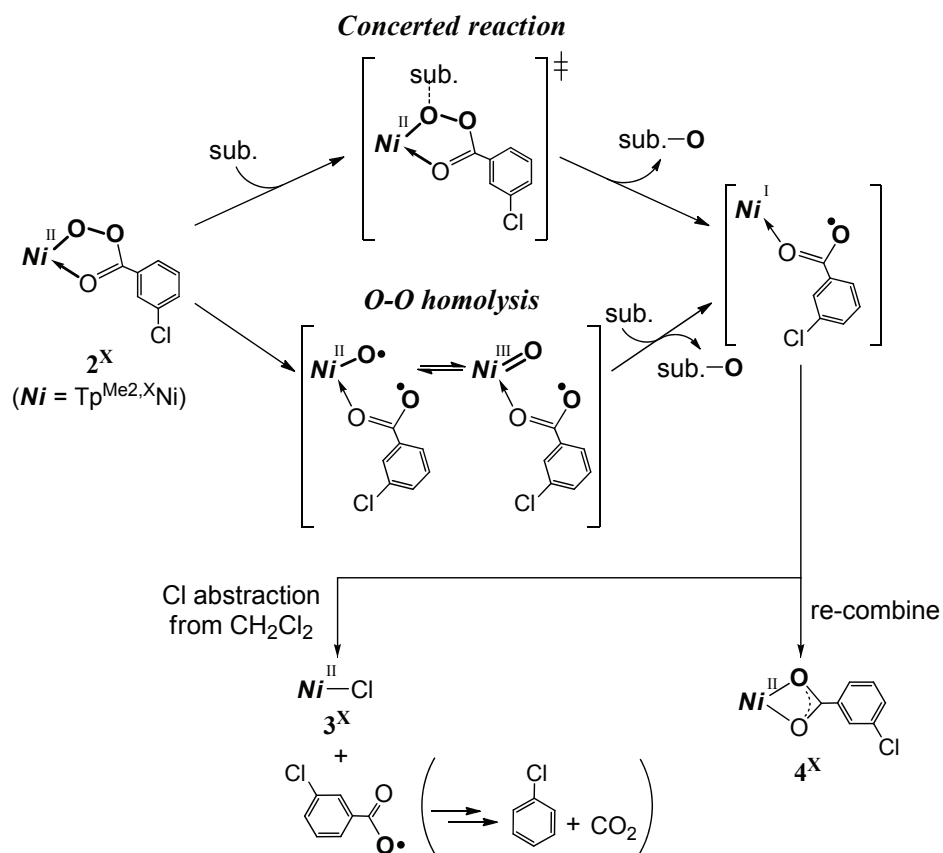
Fig. 3 UV/Vis spectra of *in situ*-generated 2^H (formed by the reaction of the dinuclear nickel(II) complex 1^H with 2 equiv of *m*CPBA) and the parent 1^H in CH_2Cl_2 at 223 K.

Fig. 4 IR spectra of the CH_2Cl_2 solutions of *in situ*-generated 2^H (formed by the reaction of the dinuclear nickel(II) complex 1^H with 2 equiv of *m*CPBA; top), the parent 1^H (bottom), and the sample once warmed to room temperature (recorded at 223 K).

Fig. 5 Decay of 2^{Br} observed by time-course UV/Vis spectra. $[2^{Br}] = 1$ mM. (a) Interval of the spectrum recording was 60 min. (b), (c) Interval of the spectrum recording was 20 min.

[View Article Online](#)

Scheme 1 Formation of the nickel(II)-acylperoxo complexes and their thermal decomposition products.



Scheme 2

Possible reaction pathways for the thermolysis of 2^{X} .

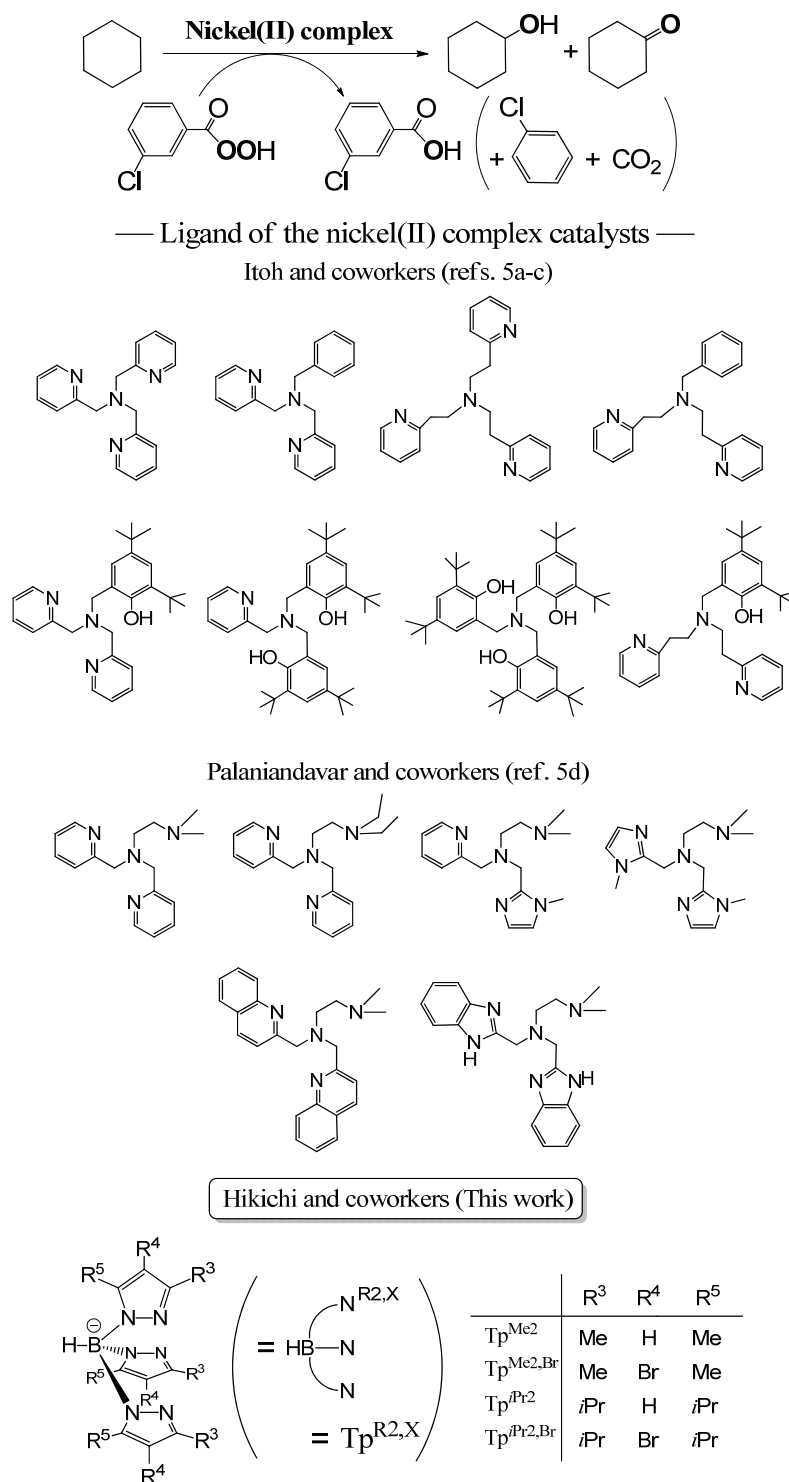
[View Article Online](#)

Fig. 1 Cyclohexane oxygenation by the Ni/*m*CPBA system and the ligands used as the support for nickel.

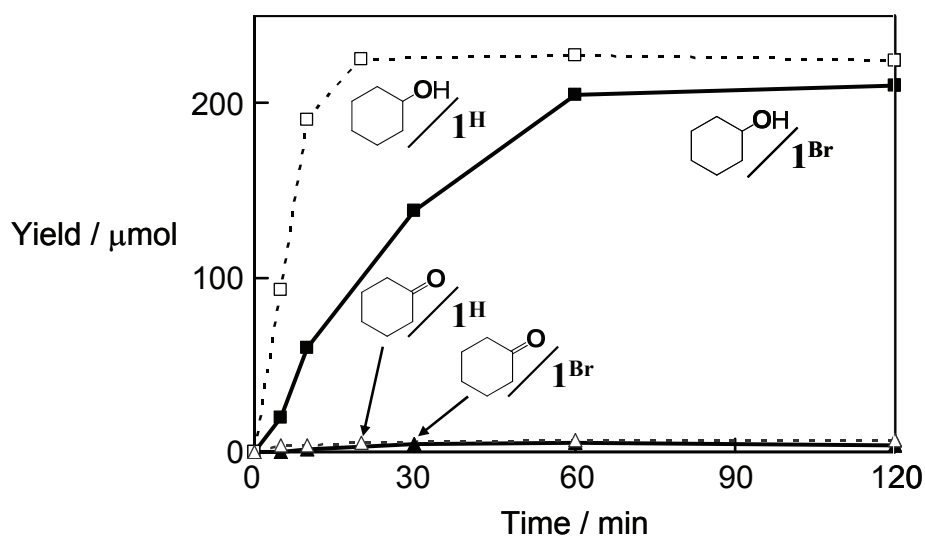


Fig. 2 Time course of cyclohexane oxidation with mCPBA mediated by 1^X under a large excess of substrate (corresponding to the entries 3 and 4 in Table 1).

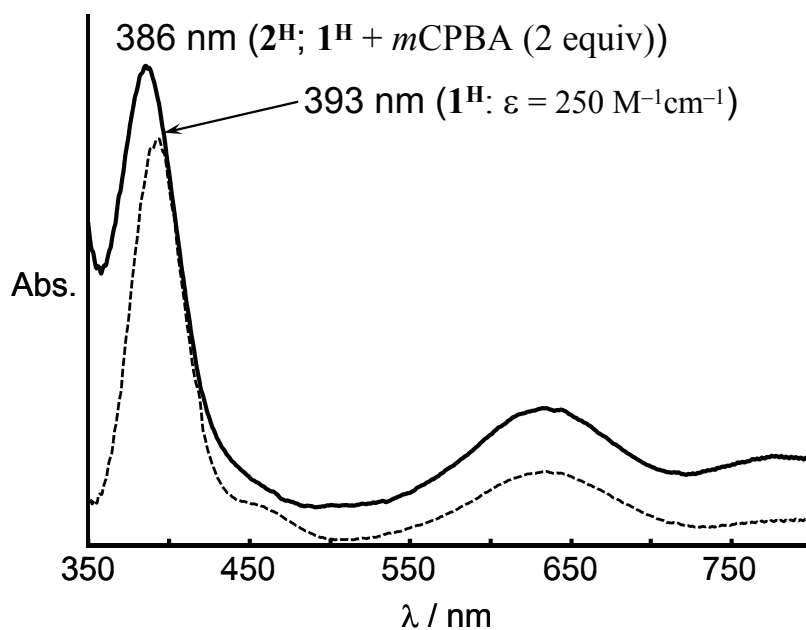
[View Article Online](#)

Fig. 3 UV/Vis spectra of *in situ*-generated 2^{H} (formed by the reaction of the dinuclear nickel(II) complex 1^{H} with 2 equiv of *m*CPBA) and the parent 1^{H} in CH_2Cl_2 at 223 K.

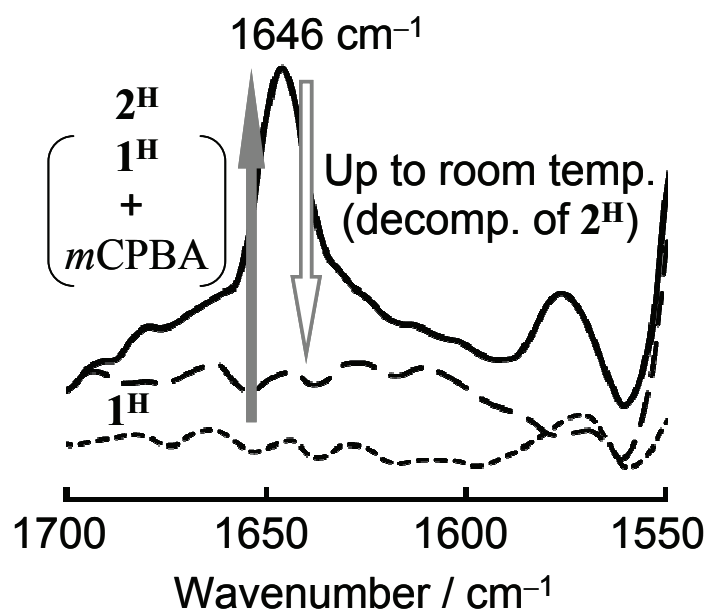


Fig. 4 IR spectra of the CH₂Cl₂ solutions of *in situ*-generated **2^H** (formed by the reaction of the dinuclear nickel(II) complex **1^H** with 2 equiv of *m*CPBA; top), the parent **1^H** (bottom), and the sample once warmed to room temperature (recorded at 223 K).

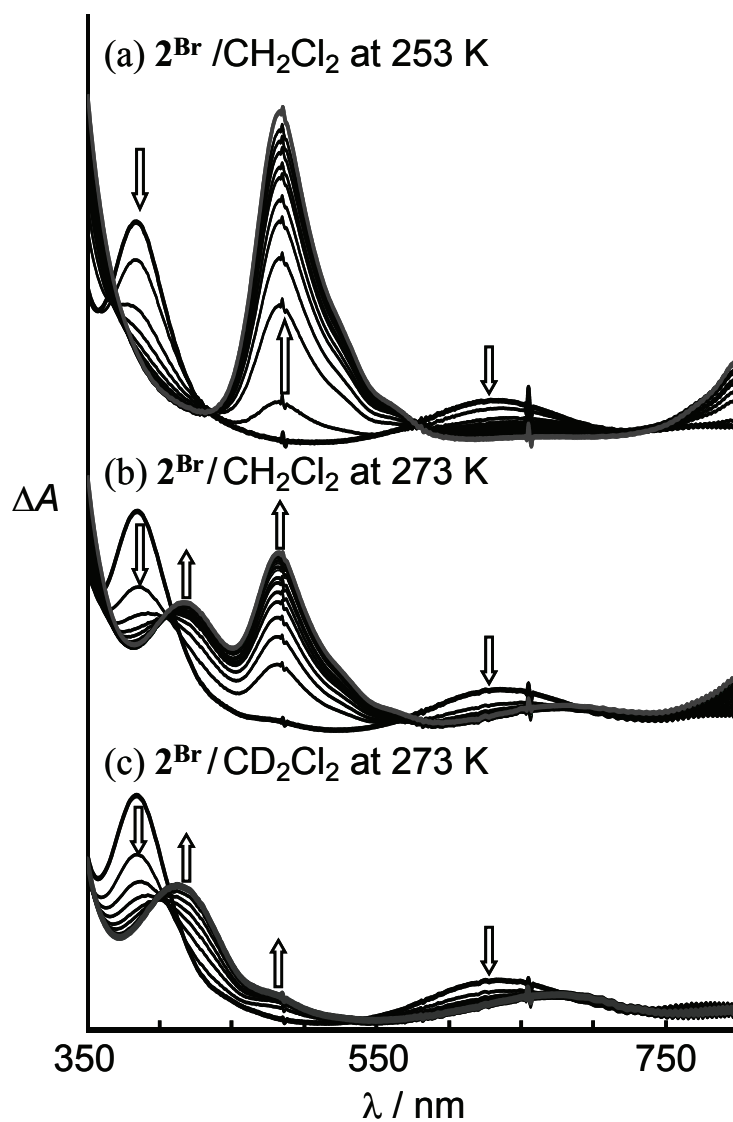
[View Article Online](#)

Fig. 5 Decay of 2^{Br} observed by time-course UV/Vis spectra. $[2^{\text{Br}}] = 1 \text{ mM}$. (a) Interval of the spectrum recording was 60 min. (b), (c) Interval of the spectrum recording was 20 min.

A table of contents entry

Nickel(II)-acylperoxo complexes, which show the potential to H atom abstraction from aliphatic C–H, have been successfully characterized.

